The arginine-ornithine transporter, *ArgT,* plays an essential role in the survival of *Brucella* in macrophages and mice.

Sushree Rekha Mallik [a,b], Kiranmai Joshi [a, b], and Girish K. Radhakrishnan [a,b*]

[a] Laboratory of Immunology and Microbial Pathogenesis, National Institute of Animal Biotechnology (NIAB), Hyderabad, Telangana, India.

[b] Regional Centre for Biotechnology (RCB), Faridabad, Haryana, India.

*Corresponding author: Girish K. Radhakrishnan (girish@niab.org.in), National Institute of Animal Biotechnology, Hyderabad-500032, India.

ABSTRACT

Brucella species are facultative intracellular bacterial pathogens causing the contagious zoonotic disease brucellosis. *Brucella* spp. infect a wide range of animals, including livestock, wild animals, and marine mammals. Brucellosis remains endemic in various parts of the world, affecting the economic growth of many countries due to its impact on public health and livestock productivity. There are no human vaccines for brucellosis, and antibiotic treatment remains inefficient. The existing animal vaccines have many disadvantages, including their residual virulence and infectivity to humans. Compared to other invasive bacterial pathogens, minimal information is available on the virulence factors of *Brucella* that enable them to survive in the host. Here, we performed a transposon-based random mutagenesis of *B. neotomae* that identified the arginine-ornithine transporter, *ArgT* as the crucial virulence determinant of *Brucella*. Deleting *ArgT* from *B. melitensis* resulted in its attenuation in macrophages, which was restored upon complementation with the *ArgT* expression plasmid. Furthermore, *Brucella* infection upregulated the host arginine transporter CAT2B expression in the macrophages. We observed that macrophages infected with Δ*ArgT*-*Brucella* produced elevated levels of nitric oxide due to the inability of Δ*ArgT Brucella* to deplete the host intracellular arginine through its transporter. Further, a defective survival of Δ*ArgT B. melitensis* was observed in the infected mice, which correlated with enhanced nitric oxide production in the infected mice. Our studies revealed that *ArgT* in *Brucella* plays a vital role in preventing intracellular killing and contributing to the chronic persistence of *Brucella* in the host. This information will help to develop improved preventive and therapeutic strategies for animal and human brucellosis.

IMPORTANCE OF THE STUDY

Brucella species are infectious intracellular bacterial pathogens causing the worldwide zoonotic disease, brucellosis, affecting animal and human health globally. There is no human vaccine for brucellosis, and antibiotic treatment is often inefficient. *Brucella* infects various phagocytes, but the mechanism by which *Brucella* resists intracellular killing remains obscure. Using a transposon-based mutagenesis screening, we identified that arginine/ornithine transporter, ArgT plays a vital role in the intracellular survival of *Brucella*. The *ArgT* knock-out *Brucella* exhibited an attenuated phenotype in macrophages and mice, which correlated with elevated levels of nitric oxide. Our experimental data suggest that

depletion of intracellular arginine through ArgT decreases nitric oxide production and protects *Brucella* from intracellular killing. This information provides crucial leads to developing improved vaccines for brucellosis.

INTRODUCTION

Brucellosis is a worldwide zoonotic disease, accounting for more than 500,000 new human infections yearly (1). Brucellosis is endemic in many parts of the developing world, posing a serious threat to the human healthcare system and constraining the economic growth of many countries (2). Despite the various control measures, brucellosis remains a major veterinary and public health problem in Asia, Africa, Latin America, the Middle East, and Europe's Mediterranean and Southeast regions (3). Brucellosis is caused by the facultative intracellular Gram-negative bacteria of the genus *Brucella*. *Brucella* infection in domestic animals results in abortion, sterility, reduced milk yield, and weak offspring. The symptoms of human brucellosis include undulating fever, chills, headache, and joint pain (4). Chronic brucellosis can lead to various complications, such as arthritis, epididymal-orchitis, endocarditis, splenic abscess, abortion, and neuro-brucellosis (5). Twelve species of *Brucella* have been identified with distinct host specificity where four *Brucella* species, such as *B. melitensis, B. abortus, B. suis*, and *B. canis*, are reported to cause human infections (6). Humans can contract the disease by ingesting contaminated dairy products, directly contacting infected animals, or inhaling *Brucella*-containing aerosols. Currently, there is no licensed vaccine for human brucellosis. The antibiotic treatment of human brucellosis is less efficient due to the prolonged duration of treatment with a combination of antibiotics, frequent relapses, and therapeutic failures (7). The available animal vaccines, such as *B. abortus* S19, RB51, and *B. melitensis* Rev1, have many disadvantages, including infectivity to humans, induction of abortion in pregnant animals, and low protection efficacy (8). Therefore, developing improved therapeutic and preventive strategies for animal and human brucellosis is essential.

Brucella can survive and replicate in both professional and nonprofessional phagocytic cells. *Brucella* exploits various host cellular processes to invade and replicate in the phagocytic cells making it a successful intracellular pathogen. *Brucella* enters the host cells through lipid rafts, resisting intracellular killing and establishing a permissive replication niche (9). *Brucella* modulates the endocytic trafficking pathways to avoid the fusion of *Brucella*-containing vacuoles with lysosomes and eventually fuses with the endoplasmic reticulum to form the replicative niche (10). *Brucella* is reported to secrete effector proteins through its Type IV Secretory System to modulate the host responses for replication and chronic persistence (11). However, there is minimal information on *Brucella* effector proteins and their host targets. Identifying the mechanisms by which Brucella subverts the host cellular process can provide new leads to developing improved vaccines and therapeutics for brucellosis.

Transposable genetic elements have been widely employed as molecular biology tools to introduce insertions into the genes for generating mutations (12). Here, we performed transposon mutagenesis of *B. neotomae* that mimics the infection dynamics of the zoonotic counterpart, *B. melitensis*. The mutagenesis screening identified the gene coding for arginine/ornithine transporter, *ArgT* as the crucial determinant of *Brucella* survival in the

macrophages. Arginine plays a vital role in the host's defense against infectious microbes as it can serve as the source for producing nitric oxide (NO). The activated macrophages undergo two major types of polarization, *viz*. M1 and M2 (13). The M1 macrophages exhibit microbicidal properties and produce pro-inflammatory cytokines whereas M2 phenotype shows anti-inflammatory and tissue repair properties (13). The M1 macrophages express nitric oxide synthase (NOS) that metabolizes arginine into NO and citrulline. The NO plays a vital role in the microbicidal property of macrophages, and citrulline will be recycled for more NO production through the citrulline-NO cycle (14). The intracellular availability of arginine determines the level of NO production. In contrast, M2 macrophages express arginase, which hydrolyses arginine into ornithine and urea, which can contribute to tissue repair and cell proliferation by producing polyamine and proline from ornithine (15). The arginase can limit NO production in M2 macrophages through hydrolysis of arginine (14).

Pathogenic microorganisms have evolved strategies to deplete the host arginine pool to attenuate the NO production that facilitates their intracellular survival. They actively transport arginine from the intracellular milieu to their cells through *ArgT*, which will be hydrolysed by the pathogen-encoded arginase (16). This will deplete the intracellular availability of arginine, leading to attenuation of NO production. We found that the Δ*ArgT*-*Brucella* presents an attenuated phenotype in macrophages and mice. We observed an enhanced production of NO in the macrophages and mice infected with Δ*ArgT B. melitensis*. Our studies revealed that *ArgT* plays an essential role in the intracellular survival of *Brucella* by attenuating the production of NO in the infected cells and animals. This information may help to develop novel vaccines and therapeutics targeting the arginine/ornithine transporter in *Brucella* and other invasive bacterial pathogens.

RESULTS

ArgT is essential for the intracellular survival of *Brucella* in macrophages.

While performing a random mutagenesis of *B. neotoma*e using *Himar1* transposon (Tn), we identified a mutant exhibiting defective survival in the macrophages. We infected RAW264.7 with Tn mutant *B. neotomae*, followed by analyzing the intracellular load of bacteria at various times post-infection. We observed defective survival of *B. neotomae* mutant at later time points in the macrophages compared to the wild type (WT) (Fig. 1A). To confirm the experimental data further, we introduced a GFP expression plasmid into the WT or Tn mutant *B. neotomae*, followed by macrophage infection studies. RAW264.7 cells were infected with GFP-expressing *Brucella*, followed by analyzing the infected cells 24 hours post-infection using a fluorescent microscope. In agreement with CFU analysis, a diminished number of mutant *B. neotomae* was observed in the macrophages as compared to the WT (Fig. 1B). These studies suggest that the Tn mutant *B. neotomae* can invade and replicate in the macrophages. However, it exhibits defective intracellular survival at the later stages of infection.

Next, we wished to identify the gene in the mutant *B. neotomae* disrupted by transposon insertion. To examine this, the genomic DNA of Tn mutant *B. neotomae* was isolated, followed by partial digestion with *Hha*1 restriction enzyme and self-ligation to obtain circular

DNA fragments (Suppl. Fig. 1B). Subsequently, the ligated product was used as the template for inverse PCR using the primers from the kanamycin-resistance (KanR) cassette to amplify the junction at which the transposon has been integrated (Suppl. Fig. 1C). The PCR amplicon was then cloned and sequenced to identify the target gene sequences (Suppl. Fig. 1D). The sequence analysis indicated that the gene, which was disrupted by *Himar1* transposon, was BMEI1022, which has been reported as an arginine/ornithine-binding periplasmic protein precursor (*ArgT*) (Suppl. Fig. 1E). The *ArgT* belongs to ATP-Binding Cassette (ABC) transporter that plays a vital role in the transportation of arginine into *Brucella* (17).

To examine the role of *ArgT* in the virulence of *Brucella*, we generated Δ*ArgT-B. neotomae* and *B. melitensis*, followed by macrophage infection studies. A homologous recombination-based gene replacement technique was employed for replacing the *ArgT* with a KanR cassette. Subsequently, the Δ*ArgT-B. neotomae* and *B. melitensis* were confirmed by PCR analysis (Suppl. Fig. 2). We also generated the Δ*ArgT+ ArgT-B. neotomae* and *B. melitensis* strains harboring an *ArgT* expression plasmid to complement the *ArgT* deficiency. To examine the infection dynamics of *Brucella* mutants, RAW264.7 were infected with WT, Δ*ArgT* or Δ*ArgT+ ArgT-Brucella*, followed by analyzing their intracellular replication at various times post-infection. In agreement with the previous observation, both Δ*ArgT-B. neotomae* and *B. melitensis* exhibited defective intracellular survival at later time points. However, this deficiency was restored in Δ*ArgT+ArgT-Brucella*, confirming the specific role of *ArgT* in the intracellular survival of *Brucella* (Fig. 1C and 1D).

Production of NO is enhanced in the macrophages infected with Δ*ArgT-Brucell*a.

Intracellular arginine act as the source for NO production to kill the microbial pathogens that are phagocytosed or invaded. However, the microbial pathogens deplete the intracellular availability of arginine through active uptake into their cells that can minimise NO production. To examine whether Δ*ArgT-Brucella* is defective in utilizing arginine, WT or Δ*ArgT* or Δ*ArgT + ArgT-B. neotomae* was inoculated into arginine deficient or arginine supplemented media, followed by measurement of OD at 600 nm at various times post-inoculation. We observed poor growth of WT or Δ*ArgT* or Δ*ArgT+ArgT-B. neotomae* in the arginine-deficient media (Fig. 2A). However, the growth defect was restored in WT or Δ*ArgT+ArgT-B. neotomae* when the arginine-deficient media was supplemented with L-arginine. In contrast, Δ*ArgT B. neotomae* exhibited poor growth in the arginine-supplemented media, indicating its inability to uptake arginine into the bacteria due to deficiency of the *ArgT* transporter.

Next, we examined the level of NO in the macrophages infected with WT or mutant *B. neotomae*. RAW264.7 cells were infected with WT, Δ*ArgT*, or Δ*ArgT + ArgT-B. neotomae*. Twenty-four hours post-infection, we analysed the levels of NO production by estimating the nitrite released into the culture supernatant. We observed an elevated level of NO in the macrophages infected with Δ*ArgT-B. neotomae* compared to the WT or Δ*ArgT +ArgT-B. neotomae* (Fig. 2B). To confirm the data further, we analysed the expression level of iNOS in the infected macrophages, which is involved in producing NO from arginine. RAW264.7 cells were infected with WT or mutant *B. neotomae* for 24 hours, followed by analysing the iNOS levels by qPCR and immunoblotting. We observed an enhanced level of iNOS

expression in the macrophages infected with Δ*ArgT-B. neotomae* compared to the WT or Δ*ArgT*+*ArgT* strain (Fig. 2C, D). As indicated before, we found a diminished load of intracellular Δ*ArgT-B. neotomae* at 24 hours post-infection, which correlates with the enhanced production of NO (Fig 1C).

To confirm the experimental data further, we analysed the production of NO in *B. neotomae*-infected macrophages, which are treated with increasing concentrations of L-arginine. RAW264.7 macrophages were treated with various concentrations of L-arginine, followed by infection with WT or Δ*ArgT* or Δ*ArgT*+ *ArgT-B. neotomae*. We found that the iNOS level and NO production were significantly enhanced in the Δ*ArgT-B. neotomae*-infected cells with increasing concentrations of L-arginine. In contrast, WT or Δ*ArgT*+*ArgT-B. neotomae* showed similar levels of iNOS expression and NO production in the infected cells (Fig. 2E and F). Consistently, the intracellular load of Δ*ArgT-B. neotomae* declined with increasing concentrations of L-arginine, indicating a direct correlation between the production of NO and its effect on the intracellular survival of *Brucella* (Fig. 2G). Next, we infected RAW264.7 cells with an increasing MOI of WT or mutant *B. neotomae*, followed by analysing the NO and iNOS levels. Increasing MOI of Δ*ArgT-B. neotomae* enhanced the expression levels of iNOS and production of NO, whereas WT or Δ*ArgT*+ *ArgT-B. neotomae* could efficiently suppress the expression of iNOS and the production of NO in the infected cells (Fig. 2H and I).

Given that *Brucella* transports arginine from the infected cells, we sought to examine whether *ArgT* and the arginase, encoded by *rocF* is upregulated in *Brucella* in the infected macrophages. To investigate this, we examined the expression levels of *Brucella ArgT* and *rocF* at various times post-infection. RAW264.7 cells were infected with *B. neotomae*, followed by analysing the expression of *ArgT* and *rocF* by qPCR. We observed elevated levels of *ArgT* and *rocF* expression at the later stages of infection in *B. neotomae* in the infected macrophages (Fig. 3A & C). To confirm the data further, we analysed the expression levels of *ArgT* and *rocF* at various concentrations of L-arginine. RAW264.7 macrophages were treated with increasing concentrations of L-arginine, followed by infection with *B. neotomae* and analysing the expression of *ArgT* and *rocF* by qPCR. We observed an enhanced *ArgT* and *rocF* expression with increasing concentrations of L-arginine (Fig. (Fig. 3B & D). Collectively, our experimental data suggest that *ArgT* and *rocF* are induced in *Brucella* for depleting the host arginine and utilizing the transported arginine for converting it into other metabolites.

Next, we analysed whether *Brucella* infection modulates the expression of the host arginine transporter, *CAT2b*, which is not constitutively expressed like *CAT1*. RAW264.7 cells were infected with *B. neotomae*, followed by analysing the endogenous levels of *CAT2b* by qPCR at various times post-infection. We observed upregulation of *CAT2b* in the macrophages at the later time point of infection (Fig 3E). The experimental data indicate that *CAT2b* is induced in the *Brucella*-infected macrophages to promote arginine transport into the infected cells for NO production.

The Δ*ArgT-B. melitensis* presents an attenuated phenotype in the infected mice.

Further, to understand the role of *ArgT in vivo*, we examined the infection dynamics of Δ*ArgT- B. melitensis* in mice. Six to eight weeks old female BALB/c mice were infected with WT or Δ*ArgT B. melitensis*, followed by analyzing the splenic load of *B. melitensis* by enumeration of CFUs at 14-day post-infection. We observed a significant reduction in the splenic load of Δ*ArgT-B. melitensis* as compared to the WT, which indicates that Δ*ArgT-B. melitensis* exhibits defective survival in the infected mice (Fig. 4A). To confirm the data further, we examined the spleen and liver weight among the mice infected with WT or Δ*ArgT-B. melitensis*. We observed increased spleen and liver weight and hepatosplenomegaly in the mice infected with WT-*B. melitensis* (Fig. 4B-D). In contrast, the spleen and liver appeared normal in the mice infected with Δ*ArgT-B. melitensis* (Fig. 4D). Further, we analyzed the iNOS expression in the spleen and levels of NO in the serum of mice infected with WT or Δ*ArgT-B. melitensis*. We found an enhanced expression of iNOS and potentiated levels of serum NO in the mice infected with Δ*ArgT-B. melitensis* as compared to the WT (Fig. 4E & F). Collectively, our experimental data suggest that Δ*ArgT-B. melitensis* is defective in suppressing the NO production, leading to the enhanced clearance of Δ*ArgT-B. melitensis* from the infected mice.

DISCUSSION

Brucella species invade and replicate in various mammalian cell types, including macrophages, dendritic cells, placental trophoblasts, microglia, and epithelial cells (18). The ability of *Brucella* to resist intracellular killing and to create a replication-permissive niche contributes to its chronic persistence in the infected host (19). Despite extensive research, more information is needed on the virulence genes and the mechanism by which *Brucella* manipulates the host cellular processes for surviving in the host. Our transposon-based screening identified *ArgT* as a virulence determinant of *Brucella* and the deletion of *ArgT* affected the survival of *Brucella* in macrophages and mice. The *ArgT* codes for arginine/ornithine-binding periplasmic protein precursor, which mediates transport of arginine/ornithine from the external environment. The arginine/ornithine transporter is present across the microbial kingdom for the uptake of arginine, which is mainly used as the energy source. Additionally, the intracellular bacterial pathogens take advantage of this transporter to deplete arginine from the host cell to neutralize the microbicidal activities of the infected cells.

Arginine is a semi-essential amino acid required for protein synthesis and plays a vital role in the innate and adaptive immune responses against infectious pathogens (14). The types of arginine metabolism determine the polarization of macrophages into pro-inflammatory, M1 macrophages and anti-inflammatory, M2 macrophages (14). In the M1 macrophages, arginine is metabolized by NOS into NO and citrulline. There are three isoforms of NOS; the inducible NOS is mainly involved in NO production and its expression is upregulated by various stimulants such as lipopolysaccharide, IFN-γ, TNF-α, and IL-1 (20). The NO free radicals produced in the M1 macrophages effectively kill the phagocytosed microbial pathogens through nitrosative stress (2). Further, NO combines with superoxide radicals and forms other reactive nitrogen species, such as peroxynitrite and nitronium ion, contributing to microbial killing (21). The M1-polarized macrophages secrete various pro-inflammatory cytokines that play a vital role in the induction of Th1-type adaptive immune responses (14). The other metabolite of arginine, citrulline, can be re-cycled to arginine for further NO

production using the citrulline-NO cycle (22). In contrast, the arginase in M2 macrophages converts arginine into ornithine and urea (14). The ornithine will be utilized for generating polyamines that regulate various tissue-repairing cellular processes such as DNA replication, cell growth, and differentiation (23). Polyamines are reported to inhibit the production of pro-inflammatory cytokines, arginine transport, and NO generation (24). Therefore, M2 macrophages function as anti-inflammatory cells and utilize arginine for tissue-repairing activities. The availability of arginine is a rate-limiting step in the production of NO by macrophages, and it is transported into the cells through cationic amino acids transporters (CAT) where *CAT1* and *CAT2b* are highly expressed in macrophages. *CAT1* is expressed constitutively, whereas *CAT2b* expression is mainly induced by the cytokines IFN-γ, IL-4, or IL-10 (25). Upregulation of *CAT2b* is associated with the induction of NOS and increased NO production in macrophages (26).

Since arginine availability is a rate-limiting step for NO production, many microbial pathogens exploit this scenario to resist the intracellular killing mediated by nitrogen free radicals. One of the microbial strategies to minimise NO production involves the depletion of arginine from the infected cells by transporting it into the microbial cells through the arginine/ornithine transporter. *ArgT* is reported to play a vital role in the intracellular survival of *S. Typhimurium* where deletion of *ArgT* resulted in enhanced bacterial clearance due to elevated levels of NO (27). Similarly, we found that deletion of *ArgT* affected the survival of *Brucella* in the macrophages and mice. The Δ*ArgT-Brucella* was defective in up-taking arginine, generating elevated NO levels in the infected macrophages and mice.

Microbial pathogens also target CAT for transporting arginine into their intracellular niche, to deplete it from the cells. Intracellular bacterial pathogens such as *Salmonella* and *E. piscicida* recruit host *CAT1* to their intracellular vacuoles to transport arginine into their replicative niche (27, 28). This helps them to utilize arginine as the energy source and minimises its availability for NO production in the infected macrophages. We observed upregulation of *CAT2b* in *Brucella*-infected macrophages, but NO production was minimal in the macrophages infected with the wild-type *Brucella* compared to the Δ*ArgT-Brucella*. This suggests that *Brucella* transports the imported arginine into the bacterial cells using *ArgT*, which facilitates the depletion of cellular arginine and diminishes NO production. An enhanced expression of *CAT1* and *CAT2b* and increased uptake of arginine have been reported in *Salmonella*-infected BMDMs and dendritic cells (27).

Arginine metabolism plays a vital role in microbial pathogenesis. The enzyme, arginase metabolizes arginine into ornithine and urea, where the ornithine is used to synthesize polyamines, which plays a vital role in microbial virulence. The microbe-encoded arginase is essential for the virulence of various pathogens, including *Leishmania*, *S. Typhimurium*, *H. pylori* and *M. tuberculosis* (27, 29). We found upregulation of arginase in *Brucella* in the culture as well as in the infected macrophages. This suggests that *Brucella* can utilize the internalized arginine to generate polyamines and other metabolites. The polyamines such as spermine can suppress the expression of pro-inflammatory cytokines and prevent the induction of iNOS in the infected macrophages (30, 31). The spermidine or spermidine is reported to induce the expression of virulence genes in bacterial pathogens to facilitate their invasion and intracellular survival (32, 33). Deletion of the arginine transporter resulted in reduced expression of virulence genes encoding T3SS in Enterohemorrhagic *Escherichia coli* (EHEC) and increased colonic arginine enhanced the virulence of *Citrobacter rodentium*

(34). The activation of arginase pathways *Edwardsiella piscicida* is reported to inhibit NLRP3 inflammasome by blocking the efflux of K+ from the macrophages (28). Further, many bacterial pathogens, including *B. abortus* encode ornithine cyclodeaminase that converts ornithine to proline, which can serve as an important source for carbon and nitrogen (35). Similarly, host arginase I or arginase II induction has been reported with other microbial pathogens, including *Leishmania major*, *Toxoplasma gondii* and *M. tuberculosis*, which enable them to minimize NO production (36, 37). These studies point out multiple roles of arginine in determining virulence, and host responses to infection, and serving as the source of nutrition during microbial infection.

The second metabolite, urea, is cleaved into carbon dioxide and ammonia by microbial urease enzyme, where ammonia can serve as a nitrogen source (38). Furthermore, ammonia generated through the action of arginase can neutralize the acidic pH in the phagolysosomes that can contribute to preventing the intracellular killing of microbial pathogens. *H. pylori* is reported to generate ammonia that increases the pH of its surroundings and favours bacterial colonisation in the stomach (39). *Brucella* also harbours urease, which can generate ammonia to suppress the microbicidal property of the infected cells. Therefore, the transport of arginine from the host cell through arginine transporters offers multiple benefits to the pathogens, such as the use of arginine as the source of energy, its depletion from the intracellular milieu to limit the production of the NO free radicals and the production of ammonia to neutralize the acidic pH in its micro-environment.

In conclusion, our experimental data indicate that *ArgT* plays an essential role in the virulence of *Brucella* in macrophages and mice. It appears that the depletion of intracellular arginine and conversion of transported arginine into other metabolites, such as polyamines and urea contribute to the intracellular survival of *Brucella* in the infected cells. Furthermore, negatively regulating the M1 polarization of macrophages by minimising NO production and the resulting suppression of pro-inflammatory cytokines can contribute to the immune evasion of *Brucella*. Our findings provide important insights into the strategies employed by *Brucella* for its chronic persistence in the infected host. Since Δ*ArgT-B. melitensis* presented an attenuated phenotype in macrophages and mice; it can serve as an ideal candidate for developing improved live-attenuated vaccines for brucellosis. Furthermore, ArgT can be targeted for developing novel therapeutic strategies for animal and human brucellosis.

MATERIALS AND METHODS

Ethical statement

Six to eight-week-old female BALB/c mice were obtained from the Animal Resource and Experimental Facility of NIAB, Hyderabad. The original breeding colonies were obtained from Jackson Labs, USA. All the experiments involving *B. melitensis* were conducted at the Biosafety Level-3/Animal -BSL3 facility of UoH-NIAB on the campus of the University of Hyderabad. The experimental protocols were approved by the Institutional Biosafety Committee (Approval number: IBSC/SEPT2019/NIAB/GR01) and Institutional Animal Ethics Committee (Approval number: IAEC/NIAB/2022/09/GKR) and BSL-3 Research Review Committee (Approval number: BSL3-Jan2022/003).

Culture of cells and Brucella

RAW264.7 murine macrophages (ATCC) were cultured in Dulbecco's Modified Eagle's Medium (Sigma) supplemented with 10% fetal bovine serum (GIBCO) and 1X penicillin-streptomycin solution (Invitrogen) and maintained at 37˚C in a humidified incubator with 5% CO2. The *B. neotomae*; 23459-5K33 was procured from ATCC. *B. melitensis* 16M was obtained from ICAR- Indian Veterinary Research Institute, Izatnagar, UP, India. *B. neotomae* and *B. melitensis* were cultured in the brucella agar or broth (BD).

Generation of transposon insertion mutants of *B. neotomae*.

The plasmid harbouring the transposable element with a kanamycin resistance cassette, pSAM-Ec was procured from (Addgene 102939). The pSAM-Ec was introduced into *B. neotomae* by electroporation and the positive colonies were selected on the brucella agar plate with kanamycin (40 µg/ml). For the preparation of electrocompetent cells, *B. neotomae* culture with an OD of 0.8-1.0 at 600 nm was collected and kept on ice for 15 minutes. The culture was then pelleted down at 8,000 rpm for 5 minutes, followed by washing the pellet with ice-cold milli-Q water thrice. Then the culture was resuspended in 100 µl of ice-cold water. To perform electroporation, 500 ng of pSAM-Ec plasmid was added into *B. neotomae* competent cells and incubated on ice for 30 minutes. The mixture was then transferred to 1mm cuvette (ice chilled) for electroporation at 1.5 kV for 5 milliseconds using an electroporator (Bio-Rad). The electroporated samples were mixed with 1 ml of SOC media and transferred into a culture tube carrying 1ml of brucella broth (BD). Subsequently, the culture was incubated with shaking for 6 hours. The culture was then pelleted down and resuspended in 100 µl of SOC broth, followed by spreading on the brucella agar plate containing kanamycin. The agar plates were incubated for 2-3 days at 37°C with 5% CO2. The colonies obtained were cultured in brucella broth with kanamycin, followed by the preparation of glycerol tubes of cultures, and stored in the -80° C freezer for future use.

Infection studies using macrophages.

RAW264.7 cells were seeded ($1x10^5$ cells/well) into 12-well plates without antibiotics and allowed to adhere overnight. Next, the cells were infected with *B. neotomae* at a multiplicity of infection (MOI) of 1000:1 or *B. melitensis* at an MOI of 200:1. After adding *Brucella*, the plates were centrifuged at 280 × g for 3 minutes to pellet-down the bacteria onto the cells. Ninety minutes post-infection the cells were washed with 1X PBS, followed by treatment with gentamycin (30 µg/ml) for 30 minutes to kill the extracellular bacteria. The cells were then washed with 1X PBS and maintained in 3 µg/ml of gentamycin-containing media until harvesting at various times post-infection for CFU analysis. To determine the CFU, the cells were lysed with 0.1% Triton X100 in PBS, followed by plating a serial dilution of the cell lysates onto brucella agar plates with kanamycin. The plates were incubated at 37° C in the presence of CO2 for 2-3 days. The colonies obtained on the plates were counted and expressed as CFU/ml.

Identification of transposon insertion site.

To identify the transposon insertion site in the genomic DNA of *B. neotomae* mutants that exhibited a defective intracellular survival, the genomic DNA of mutants were isolated using Wizard Genomic DNA Purification Kit (Promega). The isolated genomic DNA was then analysed by agarose electrophoresis and quantified using nanodrop. Subsequently, 3 µg of genomic DNA was partially digested with *Hha* I enzyme for 10 minutes. The digested products were purified using QIAquick PCR Purification Kit (Qiagen) and ligated using T4 DNA ligase (NEB) to obtain circular DNAs that contain the kanamycin-cassette and the flanking genomic DNA sequences where the transposon insertion has occurred. The ligated products were used as the template for inverse PCR using primers specific for the kanamycin cassette. The PCR products were then cloned into the pCR™4-TOPO® TA cloning vector (Thermo Fisher Scientifics), and the clones were confirmed by restriction digestion with *BamH*I. Subsequently, the clones were sequenced using M13 forward primer to identify the transposon insertion region.

Determination of nitric oxide production.

Nitrite (NO_2^-) released into the culture supernatants of *Brucella*-infected macrophages were used to determine the NO concentration with Griess Reagent Kit (Invitrogen) as per the manufacturer's instructions. To measure the NO production, macrophages were infected with WT or mutant *B. neotomae* or *B. melitensis,* as described before. Various times post-infection, the culture supernatants were harvested and mixed with N-[naphthyl] ethylenediamine dihydrochloride (0.01%; 50 µl), and sulphanilamide (0.1%; 50 µl) in 5% phosphoric acid and incubated for 1 hour at RT. The absorbance of the mixture was measured at 540 nm using a multimode plate reader (PerkinElmer). The concentration of NO was quantified using the standard curve per the manufacturer’s instructions.

To analyse NO production at various concentrations of arginine, RAW264.7 cells cultured in arginine deficient DMEM without phenol red or the same media supplemented with L-arginine (0.5, 1, and 2 mM), followed by infection with WT or mutant *Brucella* for 24 hours. The released nitrite in the culture supernatant was examined using Griess reagent as described before. The qPCR was performed using the cDNA prepared from the cells for quantifying the iNOS expression levels.

Quantitative RT-PCR analysis of gene expression.

The total RNA was isolated from the infected macrophages using RNAiso-Plus (Takara), followed by the preparation of cDNA using the Prime Script RT reagent kit (Takara) as per the manufacturer’s protocol. Data were normalized with the endogenous control, GAPDH. For analysing the *ArgT* expression, the data were normalized with the 16s rRNA of *Brucella*. The primers used for qPCR analysis are listed in Table 1.

Table. 1: List of primers used for qPCR

S. no	Gene	Sequence
1	GAPDH	F: 5′-AACGACCCCTTCATTGAC-3′ R: 5′-CCACGACATACTCAGCAC-3′

2 iNOS	F: 5′-CAGCCCAACAATACAAGATGACCC-3′ R: 5′-CAGTTCCGAGCGTCAAAGACCTGC-3′
3 *CAT2b*	F: 5′-ACAGTCCCTTCACTCTCAACA-3′ R: 5′-TACCAGGGCCGACTTTATCAG-3′
4 *ArgT*	F: 5′-CAATGCAGAAGAACCGCTCA-3′ R: 5′-GCCATCCGGCTTGATGAAAT-3′
5 16s rRNA	F: 5′-TACCAGCCCTTGACATCC-3′ R: 5′-TCATCATCCCCACCTTCCTCT-3′
6 *rocF*	F: 5′-AGCGCGGATCCATGCATTGTAAGATTCTG-3′ R: 5′-AGGCCTGCAGTCAATAGCTGATGGTCGG-3′

Generation of Δ*ArgT*-*B. neotomae* and *B. melitensis*

A homologous recombination-based gene replacement technique was used for deleting *ArgT* from the chromosomal DNA of *B. neotomae* and *B. melitensis*. To generate the knock-out construct, 1kb upstream and 1kb downstream regions of the *ArgT* gene were amplified from the genomic DNA of *B. neotomae* or *B. melitensis*. The forward and reverse for amplifying the upstream fragment harboured *Kpn*I and *BamH*I restriction enzyme sites, respectively. Similarly, the forward and reverse primers for amplifying the downstream fragment had *BamH*I and *Xho*I restriction enzyme sites, respectively. The KanR expression cassette was released from the pUC-kan-LoxP plasmid using *BamH*I restriction enzyme. Subsequently, these three fragments were purified and ligated into *Kpn*I and *Xho*I sites of pZErO1 (Thermo Fisher Scientific) vector using a 3-way ligation. The resulting *ArgT* knock-out construct was confirmed by restriction enzyme digestion and sequencing. Subsequently, the *ArgT* knock-out construct was electroporated into *B. neotomae* or *B. melitensis,* as described before. The upstream and downstream fragments in the KO plasmid recombine with the respective sequences on the chromosomal DNA of *B. neotomae,* leading to the replacement of *ArgT* gene with the KanR expression cassette. The transformed *B. neotomae* or *B. melitensis* colonies growing on kanamycin and zeocin, which indicates a single recombination event and the resulting insertion of the KO plasmid into the chromosomal DNA, were discarded. The zeocin-sensitive and kanamycin resistant Δ*ArgT*-*B. neotomae* or *B. melitensis* colonies were selected and confirmed further by PCR.

Complementation with Δ*ArgT Brucella* with *ArgT* expression plasmid.

To complement the Δ*ArgT*-*B. neotomae* or *B. melitensis* with *ArgT* expression plasmid, the *ArgT* gene was cloned into the *Brucella* expression plasmid, pNSTrcD at the *BamH*I and *Xho*I sites, respectively. Subsequently, the pNSTrcD-*ArgT* was introduced into *B. neotomae* or *B. melitensis* through electroporation, and the transformants were selected on brucella agar with chloramphenicol (40 µg/ml).

Immunoblotting.

The cells were lysed in RIPA buffer with a protease inhibitor cocktail (Pierce). The total protein in the samples was quantified using the Bradford assay (Sigma). Equal concentrations

of protein samples were mixed with 5x Laemmle buffer (Bio-Rad), and the samples were boiled for 10 min at 100° C. Next, the protein samples were run on an SDS-PAGE gel, followed by transfer onto the polyvinylidene difluoride (PVDF) membrane using a wet tank blotting system (Bio-Rad). The membrane was blocked with 5% skimmed milk in Tris-buffered saline with Tween-20 (TBST; Cell Signalling Technology) for 1 hour, followed by incubation with the respective primary antibody overnight at 4° C. Next, the membrane was washed 3 times with TBST and incubated with horseradish peroxidase (HRP)-conjugated secondary antibody. The primary or secondary antibody was diluted in 5% skimmed milk in TBST. Finally, the membrane was washed thrice with TBST and incubated with Super Signal West Pico or Femto chemiluminescent substrate (Pierce). The signals were captured using a chemi-documentation system (Syngene). The antibody dilutions used are listed in Table 2.

Table. 2: List of antibodies used in the study.

S. no	Antibody	Source	Dilution
1	iNOS	Cell Signalling Technology	1:1000
2	Anti-actin HRP-conjugated	Sigma Aldrich	1:25,000
3	Anti-rabbit HRP-conjugated	Cell Signalling Technology	1:5,000

Generation of *B. neotomae* expressing GFP for fluorescence microscopy.

To generate *B. neotomae* expressing green fluorescent protein (GFP), *Brucella* expression plasmid (pNSTrcD) harbouring GFP was electroporated into wild-type or mutant *B. neotomae* as described before. The transformants were selected on a brucella agar plate containing chloramphenicol (40 µg/mL). For fluorescence microscopy, RAW264.7 cells were seeded into glass-bottom imaging dish (5 x 10^4/ dish) and allowed to adhere overnight. Next, the cells were infected with WT or mutant *B. neotomae*-GFP for 24 hours. Subsequently, the infected cells were fixed with 4% paraformaldehyde in PBS, followed by staining the nuclei with Hoechst stain (Thermo Fisher Scientific). The images were captured using a fluorescent microscope (Carl Zeiss) at 20X magnification. Total of twelve fields were observed for each sample.

Mice infection

Six- to seven-week-old female BALB/c mice (6 mice/group) were injected intraperitoneally with WT, or Δ*ArgT-B. melitensis* (2×10^6 CFU/mice). Fourteen days post-infection, the mice were euthanized, followed by the collection of liver and spleen aseptically. The weight of the spleen and liver were measured using a digital weighing balance. For CFU enumeration, the spleens were homogenized in 1X PBS (1 ml) using the bead beater, followed by clarifying the homogenates by centrifugation. Subsequently, the homogenates were serially diluted in 1X PBS and plated onto the brucella agar plates. The plates were incubated at 37° C with 5% CO2 for 2-3 days, followed by enumeration of CFU. To examine the iNOS levels, mice (5 mice/group) were infected with WT or mutant *B. melitensis* as described before. Fourteen days post-infection, the spleens were collected, followed by isolation of total RNA and cDNA preparation. Subsequently, the iNOS levels were determined by qPCR analysis. The

serum prepared from the infected or control mice was used for analysing the NO production by Griess reagent.

Statistical analysis.

Data are shown as the mean of triplicates ± standard error of the mean (SEM). The levels of significance were set at $P < 0.05$. GraphPad Prism 7.0 software was for the statistical analysis of experimental data. Data are shown as the mean ± standard error of the mean (SEM). Statistical significance was determined by t-tests (two-tailed) for pairwise comparison. A one-way analysis of variance (ANOVA) Dunnett hypothesis test was used to analyse the data involving more than two samples.

ACKNOWLEDGMENTS

We thank the National Institute of Animal Biotechnology for providing the funding, and experimentation facility. We acknowledge the BSL3/A-BSL3 facility of UoH-NIAB for experiments with *B. melitensis*. SRM acknowledges the research fellowship from the University Grant Commission (UGC).

ABBREVIATION

iNOS: Induced nitric oxide synthase

NO: Nitric Oxide

Cat: Cationic amino acid transporter

ArgT: Arginine ornithine binding transporter protein

Δ*ArgT*: Arginine ornithine binding transporter protein knock-out

rocF: Arginase

AUTHOR'S CONTRIBUTION

GR conceived and designed the study. SRM and KJ performed the experiments and analysed the experimental data. GR and SRM prepared the manuscript. All authors reviewed the results and approved the final version of the manuscript.

COMPETING INTERESTS

The authors declare that they have no conflicts of interest with the contents of this article.

Figure 1. Δ*ArgT Brucella* exhibits defective intracellular survival in the macrophages. (A) RAW264.7 cells were infected with wild-type (WT-Bneo) or Transposon-insertional mutant of *B. neotomae* (C13-Bneo), followed by quantification of the intracellular load of bacteria by enumeration of CFU at indicated times post-infection. **(B)** Fluorescence microscopy images showing the intracellular load of WT-Bneo or C13-Bneo expressing GFP. RAW264.7 cells were infected with GFP-expressing *Brucella*, followed by analysing the infected cells using a fluorescent microscope at 24 hours post-infection. The cell nuclei were stained with DAPI (blue). Scale bar, 50 μm. The images are representative of three independent experiments where 12 fields were captured and analysed for each experiment. The right panel indicates the quantification of the number of intracellular bacteria using ImageJ software. **(C)** Macrophage infection studies using WT (WT-Bneo) or Δ*ArgT-B. neotomae* (Δ*ArgT*-Bneo) *or* Δ*ArgT-B. neotomae* complemented with *ArgT* expression plasmid (Δ*ArgT*+*ArgT*-Bneo). RAW264.7 cells were infected with indicated strains of *B. neotomae*, followed by the enumeration of CFUs at various times post-infection**.** (**D**) The intracellular load of WT (WT-BmeI) or Δ*ArgT B. melitensis* (Δ*ArgT*-BmeI) or Δ*ArgT*+*ArgT B. melitensis* (Δ*ArgT*+*ArgT*-BmeI) in RAW264.7 cells at indicated times post-infection. The data are presented as the mean ± SEM from at least three independent experiments (***, $P < 0.001$).

Figure 2. The macrophages infected with Δ*ArgT-B. neotomae* produced elevated levels of nitric oxide (NO). (A) Growth dynamics of WT (WT-Bneo) or Δ*ArgT-B. neotomae* (Δ*ArgT*-Bneo) or Δ*ArgT*+*ArgT-B. neotomae* (Δ*ArgT*+*ArgT*-Bneo) in the media with or without arginine. The indicated *B. neotomae* strains were inoculated into the arginine (-) or arginine (-) media supplemented with L-arginine. The OD was analyzed at indicated times post-inoculation**. (B)** Δ*ArgT-B. neotomae*-infected macrophages produce elevated levels of NO. RAW264.7 cells were infected with WT-Bneo or Δ*ArgT*-Bneo or Δ*ArgT*+*ArgT*-Bneo, followed by quantification of NO levels at 24 hours post-infection**. (C&D)** Enhanced level of iNOS expression in the macrophages infected with Δ*ArgT*-Bneo. RAW264.7 cells were infected with WT-Bneo or Δ*ArgT*-Bneo or Δ*ArgT*+*ArgT*-Bneo, followed by quantification of iNOS mRNA levels by qPCR and iNOS protein levels by immunoblotting at 24 hours post-infection. The membranes were probed with anti-iNOS antibody to detect the endogenous levels of iNOS. Actin served as the loading control. The right panel indicates the densitometry of iNOS bands, which were normalized with actin. The immunoblot is representative of three different experiments. **(E & F)** The levels of *Brucella*-induced NO and iNOS in the macrophages grew with increasing L-arginine concentrations. RAW264.7 cells were infected with WT-Bneo or Δ*ArgT*-Bneo or Δ*ArgT*+*ArgT*-Bneo in DMEM (-) arginine or DMEM (-) arginine supplemented with indicated concentrations of L-arginine, followed by quantification of NO levels in the culture supernatants, iNOS expression levels in the cells

and determination of intracellular load of *B. neotomae* strains **(G)** at 24 hours post-infection. **(H&I)** The levels of NO and iNOS in the macrophages infected with various MOI of *Brucella*. RAW264.7 cells were infected with an increasing MOI of WT-Bneo or Δ*ArgT*-Bneo or Δ*ArgT*+*ArgT*-Bneo, followed by quantification of NO levels in the culture supernatants and iNOS expression levels in the cells at 24 hours post-infection. The data are presented as the mean ± SEM from at least three independent experiments (*, $P < 0.05$; **, $P < 0.01$; ***, $P < 0.001$; ****, $P < 0.0001$).

Figure 3. (A, B) Expression levels of *ArgT* and *rocF* in *B. neotomae* at various time points of infection. RAW264.7 cells were infected with WT-*B. neotomae*, followed by harvesting the infected cells at indicated time points and quantification of expression levels of *ArgT* and *rocF* of *B. neotomae* by qPCR. **(C, D)** Expression levels of *ArgT* and *rocF* in *B. neotomae* with increasing concentrations of arginine. RAW264.7 cells were infected with WT-*B. neotomae* in DMEM (-) arginine or DMEM (-) arginine supplemented with indicated concentrations of L-arginine for 24 hours, followed by quantification of *ArgT* and *rocF* expression levels by qPCR. The qPCR data were normalized with 16s rRNA, and relative mRNA expression was quantified with respect to uninfected macrophages for the corresponding time point of infection. **(E)** Upregulation of cationic amino acid transporter in the *Brucella*-infected macrophages**.** RAW264.7 macrophages were infected with WT-*B. neotomae* (WT-Bneo), followed by quantification of the expression levels of *CAT2b* at indicated time points by qPCR. The data were normalized with GAPDH, and relative mRNA expression was determined with respect to the uninfected macrophages for each time point of infection. The data are presented as the mean ± SEM from at least three independent experiments (*, $P < 0.05$; **, $P < 0.01$; ***, $P < 0.001$; ****, $P < 0.0001$).

Figure 4. Δ*ArgT*-*B. melitensis* presents an attenuated phenotype in mice. (A) Six to eight weeks old BALB/c mice were infected with WT (WT-BmeI) or Δ*ArgT*-*B. melitensis* (Δ*ArgT*-BmeI). Fourteen days post-infection, the mice were sacrificed, followed by the collection of blood, spleens, and liver. The spleens were homogenized, followed by enumeration of CFU to determine the splenic load of WT or Δ*ArgT*-BmeI. **(A)** The weights of the spleen **(B)** and liver **(C)** of mice infected with WT or Δ*ArgT*-BmeI. **(D)** The photograph showing the spleen of mice infected with WT or Δ*ArgT*-BmeI. PBS was used as the negative control. **(E&F)** Levels of NO and iNOS in the mice infected with WT or Δ*ArgT*-BmeI. The NO levels were determined in the serum of infected mice using Griess reagent, and iNOS expression levels were examined in the spleen by qPCR analysis. The data were normalized with GAPDH, and relative mRNA expression was determined with respect to the group treated with PBS. The data are presented as the mean ± SEM from at least two independent experiments ($P < 0.01$; ***, $P < 0.001$; ****, $P < 0.0001$).

593

594

595

596

597 **REFERENCES**

598 1. Gwida M, Al Dahouk S, Melzer F, Rosler U, Neubauer H, Tomaso H. 2010. Brucellosis -
599 regionally emerging zoonotic disease? Croat Med J 51:289-95.
600 2. Franc KA, Krecek RC, Hasler BN, Arenas-Gamboa AM. 2018. Brucellosis remains a neglected
601 disease in the developing world: a call for interdisciplinary action. BMC Public Health 18:125.
602 3. Nicoletti P. 2010. Brucellosis: past, present and future. Prilozi 31:21-32.
603 4. Khan MZ, Zahoor M. 2018. An Overview of Brucellosis in Cattle and Humans, and its
604 Serological and Molecular Diagnosis in Control Strategies. Trop Med Infect Dis 3.
605 5. Corbel MJ. 1997. Brucellosis: an overview. Emerg Infect Dis 3:213-21.
606 6. Al Dahouk S, Kohler S, Occhialini A, Jimenez de Bagues MP, Hammerl JA, Eisenberg T,
607 Vergnaud G, Cloeckaert A, Zygmunt MS, Whatmore AM, Melzer F, Drees KP, Foster JT,
608 Wattam AR, Scholz HC. 2017. Brucella spp. of amphibians comprise genomically diverse
609 motile strains competent for replication in macrophages and survival in mammalian hosts.
610 Sci Rep 7:44420.
611 7. Ariza J, Bosilkovski M, Cascio A, Colmenero JD, Corbel MJ, Falagas ME, Memish ZA, Roushan
612 MR, Rubinstein E, Sipsas NV, Solera J, Young EJ, Pappas G, International Society of C,
613 Institute of Continuing Medical Education of I. 2007. Perspectives for the treatment of
614 brucellosis in the 21st century: the Ioannina recommendations. PLoS Med 4:e317.
615 8. Hoffman T, Rock K, Mugizi DR, Muradrasoli S, Lindahl-Rajala E, Erume J, Magnusson U,
616 Lundkvist A, Boqvist S. 2016. Molecular detection and characterization of Brucella species in
617 raw informally marketed milk from Uganda. Infect Ecol Epidemiol 6:32442.
618 9. Gonzalez-Espinoza G, Arce-Gorvel V, Memet S, Gorvel JP. 2021. Brucella: Reservoirs and
619 Niches in Animals and Humans. Pathogens 10.
620 10. Celli J. 2019. The Intracellular Life Cycle of Brucella spp. Microbiol Spectr 7.
621 11. Ke Y, Wang Y, Li W, Chen Z. 2015. Type IV secretion system of Brucella spp. and its effectors.
622 Front Cell Infect Microbiol 5:72.
623 12. Picardeau M. 2010. Transposition of fly mariner elements into bacteria as a genetic tool for
624 mutagenesis. Genetica 138:551-8.
625 13. Mosser DM, Edwards JP. 2008. Exploring the full spectrum of macrophage activation. Nat
626 Rev Immunol 8:958-69.
627 14. Rath M, Muller I, Kropf P, Closs EI, Munder M. 2014. Metabolism via Arginase or Nitric Oxide
628 Synthase: Two Competing Arginine Pathways in Macrophages. Front Immunol 5:532.
629 15. Novak ML, Koh TJ. 2013. Macrophage phenotypes during tissue repair. J Leukoc Biol 93:875-
630 81.
631 16. Munder M. 2009. Arginase: an emerging key player in the mammalian immune system. Br J
632 Pharmacol 158:638-51.
633 17. Jenner DC, Dassa E, Whatmore AM, Atkins HS. 2009. ATP-Binding Cassette Systems of
634 Brucella. Comp Funct Genomics 2009:354649.

635 18. Martirosyan A, Gorvel JP. 2013. Brucella evasion of adaptive immunity. Future Microbiol
636 8:147-54.
637 19. Guo X, Zeng H, Li M, Xiao Y, Gu G, Song Z, Shuai X, Guo J, Huang Q, Zhou B, Chu Y, Jiao H.
638 2023. The mechanism of chronic intracellular infection with Brucella spp. Front Cell Infect
639 Microbiol 13:1129172.
640 20. Modolell M, Corraliza IM, Link F, Soler G, Eichmann K. 1995. Reciprocal regulation of the
641 nitric oxide synthase/arginase balance in mouse bone marrow-derived macrophages by TH1
642 and TH2 cytokines. Eur J Immunol 25:1101-4.
643 21. Prolo C, Alvarez MN, Radi R. 2014. Peroxynitrite, a potent macrophage-derived oxidizing
644 cytotoxin to combat invading pathogens. Biofactors 40:215-25.
645 22. Mori M, Gotoh T. 2004. Arginine metabolic enzymes, nitric oxide and infection. J Nutr
646 134:2820S-2825S; discussion 2853S.
647 23. Pegg AE, McCann PP. 1982. Polyamine metabolism and function. Am J Physiol 243:C212-21.
648 24. Latour YL, Gobert AP, Wilson KT. 2020. The role of polyamines in the regulation of
649 macrophage polarization and function. Amino Acids 52:151-160.
650 25. Gogoi M, Datey A, Wilson KT, Chakravortty D. 2016. Dual role of arginine metabolism in
651 establishing pathogenesis. Curr Opin Microbiol 29:43-8.
652 26. Kawahara K, Gotoh T, Oyadomari S, Kajizono M, Kuniyasu A, Ohsawa K, Imai Y, Kohsaka S,
653 Nakayama H, Mori M. 2001. Co-induction of argininosuccinate synthetase, cationic amino
654 acid transporter-2, and nitric oxide synthase in activated murine microglial cells. Brain Res
655 Mol Brain Res 90:165-73.
656 27. Das P, Lahiri A, Lahiri A, Sen M, Iyer N, Kapoor N, Balaji KN, Chakravortty D. 2010. Cationic
657 amino acid transporters and Salmonella Typhimurium ArgT collectively regulate arginine
658 availability towards intracellular Salmonella growth. PLoS One 5:e15466.
659 28. Jiang J, Wang W, Sun F, Zhang Y, Liu Q, Yang D. 2021. Bacterial infection reinforces host
660 metabolic flux from arginine to spermine for NLRP3 inflammasome evasion. Cell Rep
661 34:108832.
662 29. Boitz JM, Gilroy CA, Olenyik TD, Paradis D, Perdeh J, Dearman K, Davis MJ, Yates PA, Li Y,
663 Riscoe MK, Ullman B, Roberts SC. 2017. Arginase Is Essential for Survival of Leishmania
664 donovani Promastigotes but Not Intracellular Amastigotes. Infect Immun 85.
665 30. Moyat M, Velin D. 2014. Immune responses to Helicobacter pylori infection. World J
666 Gastroenterol 20:5583-93.
667 31. Bussiere FI, Chaturvedi R, Cheng Y, Gobert AP, Asim M, Blumberg DR, Xu H, Kim PY, Hacker
668 A, Casero RA, Jr., Wilson KT. 2005. Spermine causes loss of innate immune response to
669 Helicobacter pylori by inhibition of inducible nitric-oxide synthase translation. J Biol Chem
670 280:2409-12.
671 32. Di Martino ML, Campilongo R, Casalino M, Micheli G, Colonna B, Prosseda G. 2013.
672 Polyamines: emerging players in bacteria-host interactions. Int J Med Microbiol 303:484-91.
673 33. Eriksson S, Lucchini S, Thompson A, Rhen M, Hinton JC. 2003. Unravelling the biology of
674 macrophage infection by gene expression profiling of intracellular Salmonella enterica. Mol
675 Microbiol 47:103-18.
676 34. Menezes-Garcia Z, Kumar A, Zhu W, Winter SE, Sperandio V. 2020. l-Arginine sensing
677 regulates virulence gene expression and disease progression in enteric pathogens. Proc Natl
678 Acad Sci U S A 117:12387-12393.
679 35. Kim J, Mayfield JE. 1997. Brucella abortus arginase and ornithine cyclodeaminase genes are
680 similar to Ti plasmid arginase and ornithine cyclodeaminase. Biochim Biophys Acta 1354:55-
681 7.
682 36. El Kasmi KC, Qualls JE, Pesce JT, Smith AM, Thompson RW, Henao-Tamayo M, Basaraba RJ,
683 Konig T, Schleicher U, Koo MS, Kaplan G, Fitzgerald KA, Tuomanen EI, Orme IM, Kanneganti
684 TD, Bogdan C, Wynn TA, Murray PJ. 2008. Toll-like receptor-induced arginase 1 in

685 macrophages thwarts effective immunity against intracellular pathogens. Nat Immunol
686 9:1399-406.
687 37. Iniesta V, Carcelen J, Molano I, Peixoto PM, Redondo E, Parra P, Mangas M, Monroy I,
688 Campo ML, Nieto CG, Corraliza I. 2005. Arginase I induction during Leishmania major
689 infection mediates the development of disease. Infect Immun 73:6085-90.
690 38. Mobley HL, Island MD, Hausinger RP. 1995. Molecular biology of microbial ureases.
691 Microbiol Rev 59:451-80.
692 39. Zhang X, Zhang J, Zhang R, Guo Y, Wu C, Mao X, Guo G, Zhang Y, Li D, Zou Q. 2013.
693 Structural, enzymatic and biochemical studies on Helicobacter pylori arginase. Int J Biochem
694 Cell Biol 45:995-1002.

695

696

Fig. 1

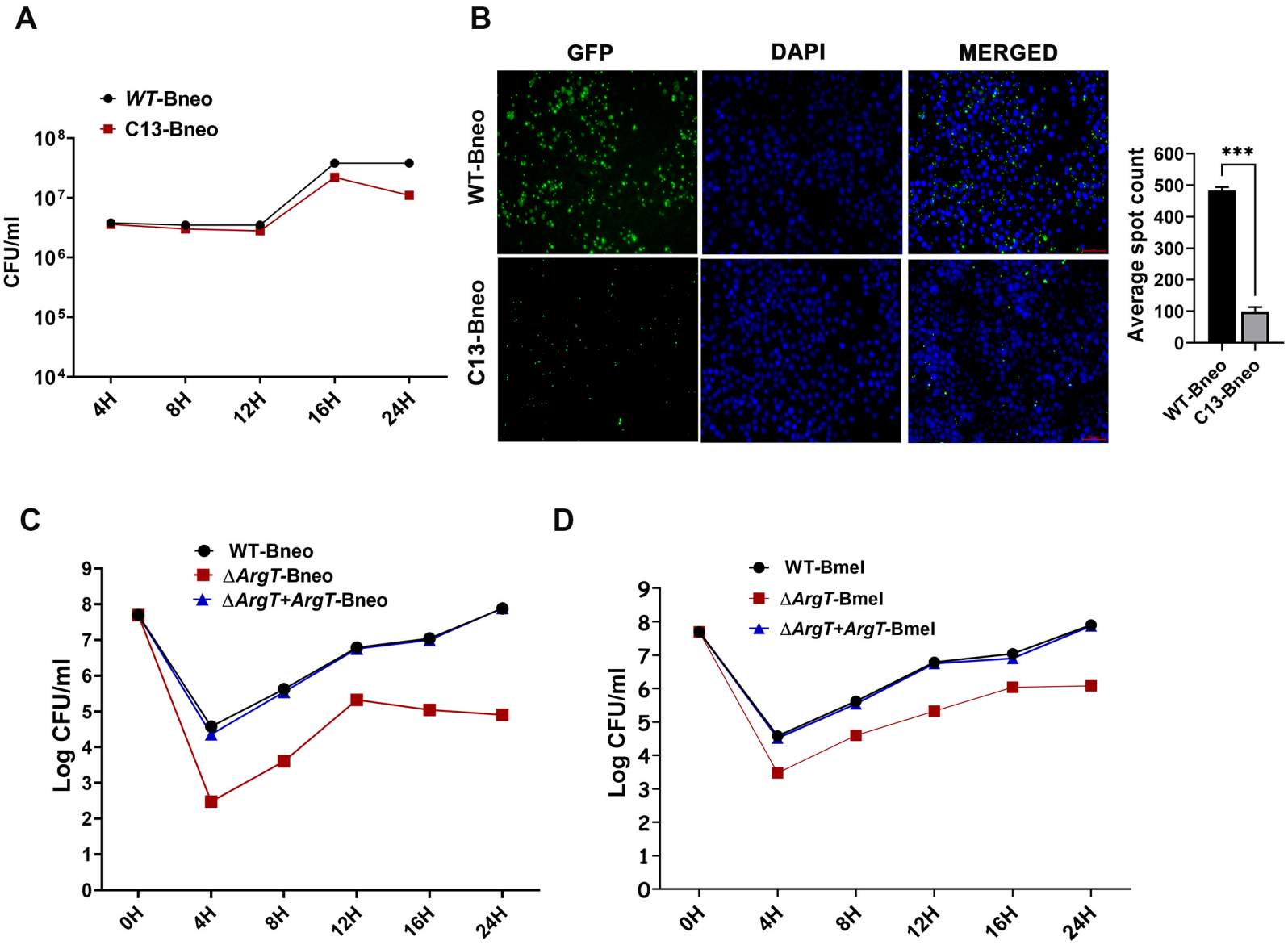
A
WT-Bneo
C13-Bneo
CFU/ml
4H
8H
12H
16H
24H
B
GFP
DAPI
MERGED
WT-Bneo
C13-Bneo
Average spot count
***
C
WT-Bneo
ΔArgT-Bneo
ΔArgT+ArgT-Bneo
Log CFU/ml
0H
D
WT-BmeI
ΔArgT-BmeI
ΔArgT+ArgT-BmeI

Fig. 2

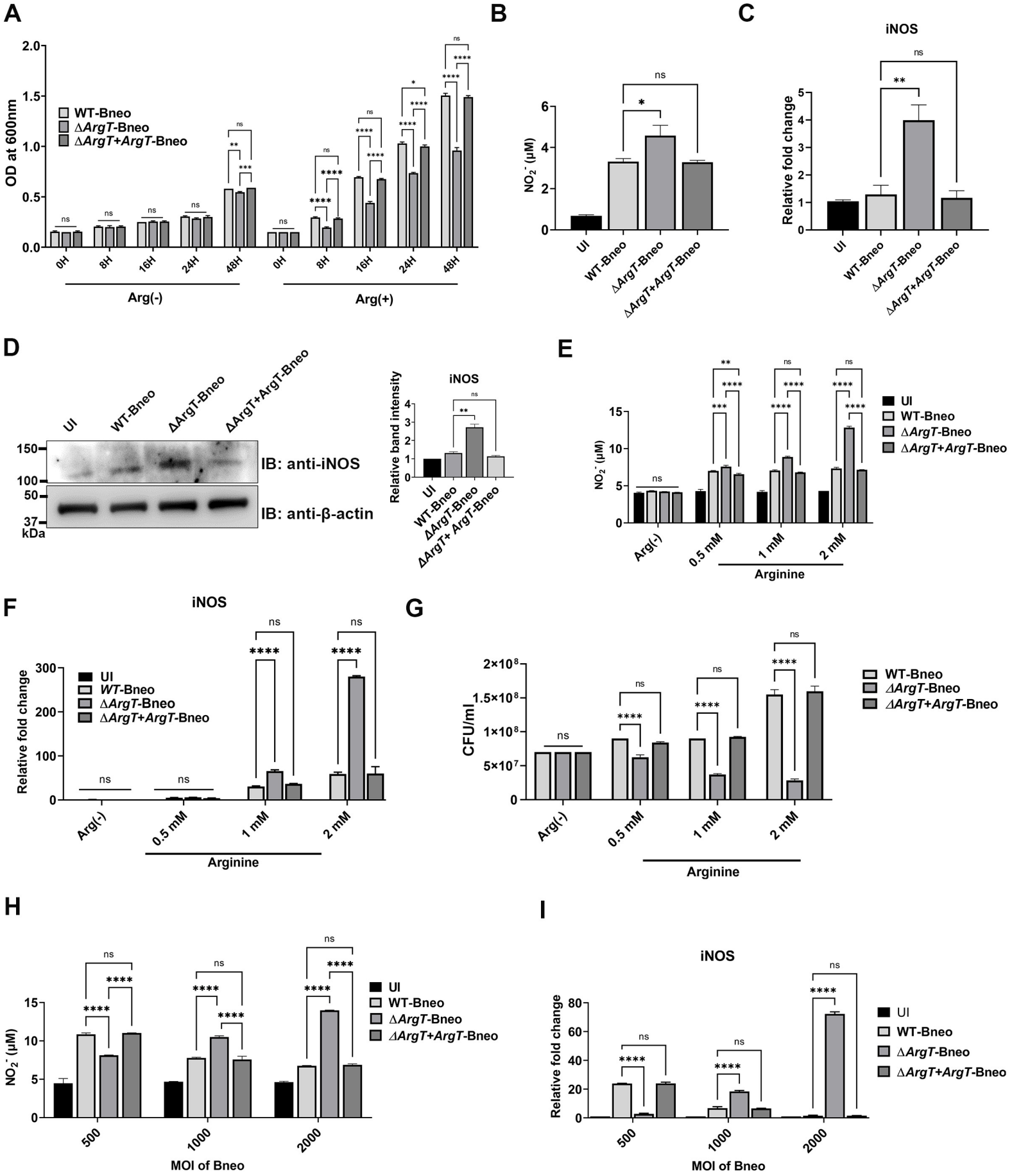
A
OD at 600nm
WT-Bneo
ΔArgT-Bneo
ΔArgT+ArgT-Bneo
0H
8H
16H
24H
48H
Arg(-)
Arg(+)
B
NO2- (μM)
UI
WT-Bneo
ΔArgT-Bneo
ΔArgT+ArgT-Bneo
C
iNOS
Relative fold change
D
UI
WT-Bneo
ΔArgT-Bneo
ΔArgT+ArgT-Bneo
IB: anti-iNOS
IB: anti-β-actin
kDa
Relative band intensity
E
Arg(-)
0.5 mM
1 mM
2 mM
Arginine
F
Relative fold change
G
CFU/ml
H
MOI of Bneo
I

Fig. 3

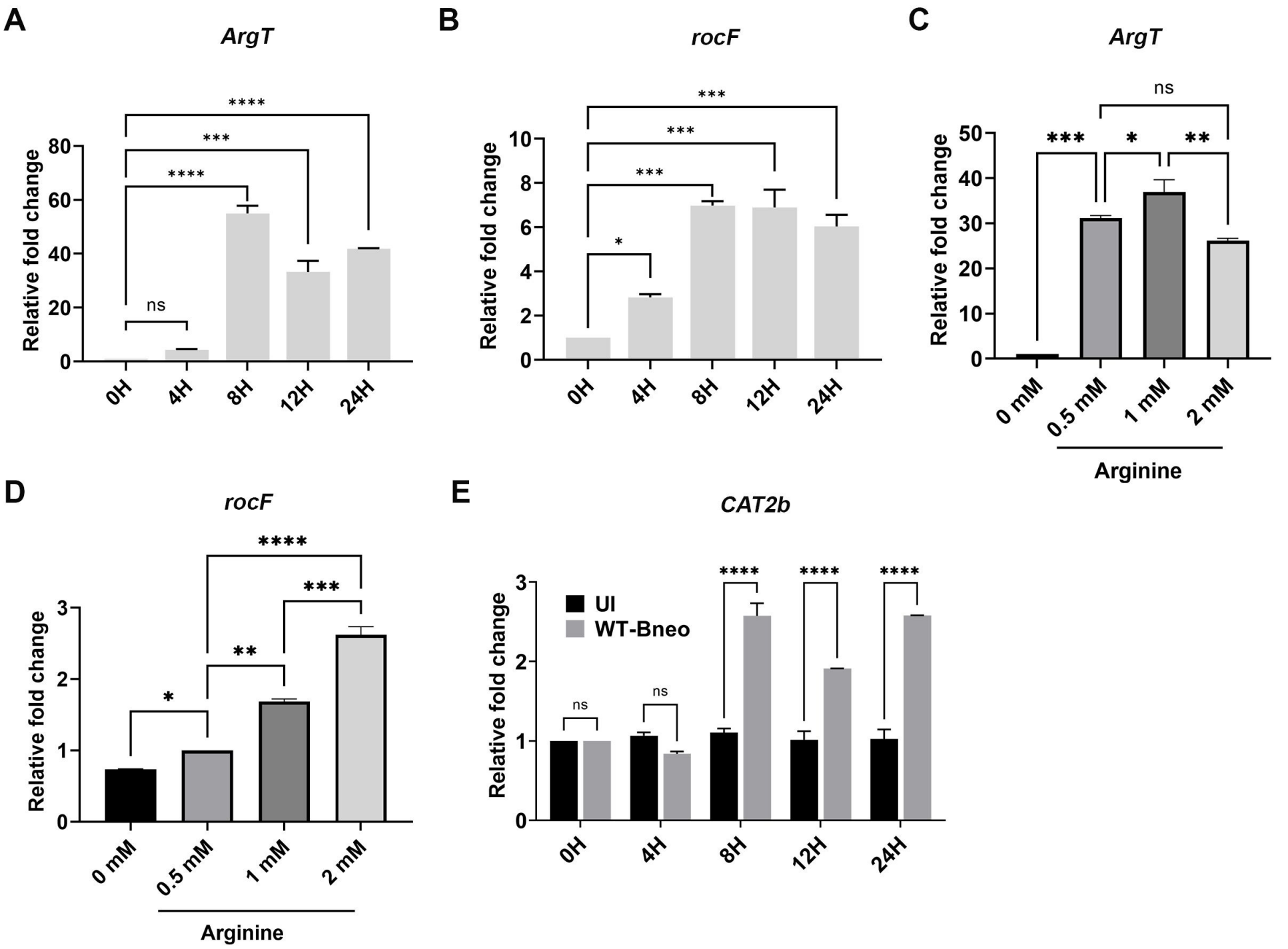
A
ArgT
Relative fold change
0
20
40
60
80
ns
****
***
****
0H
4H
8H
12H
24H
B
rocF
Relative fold change
0
2
4
6
8
10
*
***
***
***
0H
4H
8H
12H
24H
C
ArgT
Relative fold change
0
10
20
30
40
50
***
*
**
ns
0 mM
0.5 mM
1 mM
2 mM
Arginine
D
rocF
Relative fold change
0
1
2
3
*
**
***
****
0 mM
0.5 mM
1 mM
2 mM
Arginine
E
CAT2b
Relative fold change
0
1
2
3
UI
WT-Bneo
ns
ns
****
****
****
0H
4H
8H
12H
24H

Fig. 4

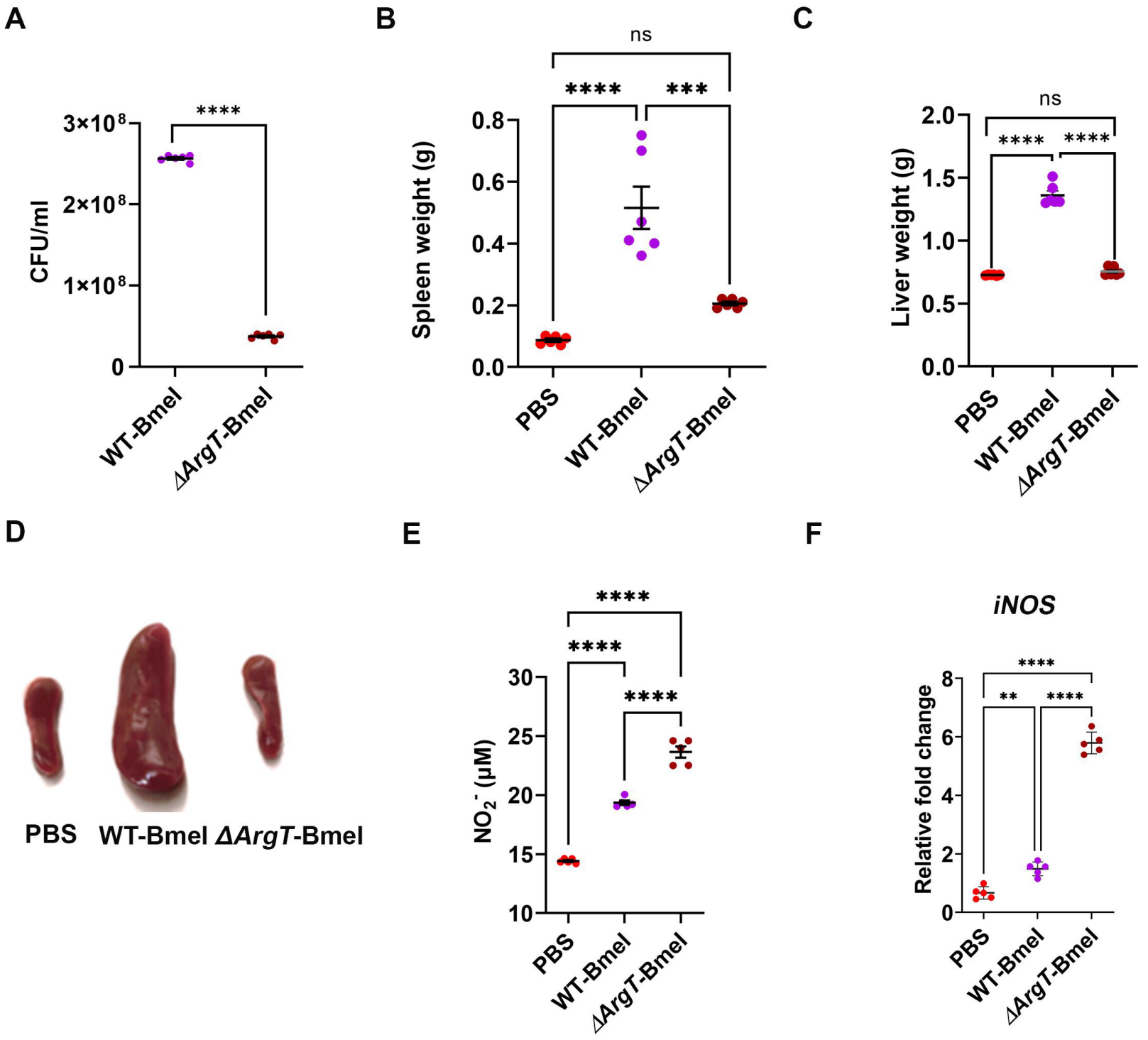
A
CFU/ml
3×10⁸
2×10⁸
1×10⁸
0
****
WT-Bmel
ΔArgT-Bmel
B
Spleen weight (g)
0.8
0.6
0.4
0.2
0.0
ns
****
***
PBS
WT-Bmel
ΔArgT-Bmel
C
Liver weight (g)
2.0
1.5
1.0
0.5
0.0
ns
****
****
PBS
WT-Bmel
ΔArgT-Bmel
D
PBS
WT-Bmel ΔArgT-Bmel
E
NO2- (μM)
30
25
20
15
10
****
****
****
PBS
WT-Bmel
ΔArgT-Bmel
F
iNOS
Relative fold change
8
6
4
2
0
****
**
****
PBS
WT-Bmel
ΔArgT-Bmel